P-selectin drives complement attack on endothelium during intravascular hemolysis in TLR-4/heme-dependent manner

Nicolas S. Merle[a,b,c], Romain Paule[a,c,d], Juliette Leon[a,b,c], Marie Daugan[a,b,c], Tania Robe-Rybkine[a,b,c], Victoria Poillerat[a,b,c], Carine Torset[a,b,c], Véronique Frémeaux-Bacchi[a,b,c,e], Jordan D. Dimitrov[a,b,c,1], and Lubka T. Roumenina[a,b,c,1]

[a]Centre de Recherche des Cordeliers, UMR_S 1138, INSERM, F-75006 Paris, France; [b]Centre de Recherche des Cordeliers, Sorbonne Universités, F-75006 Paris, France; [c]Centre de Recherche des Cordeliers, Université Paris Descartes, Sorbonne Paris Cité, F-75006 Paris, France; [d]Service de Médecine Interne, Hôpital Foch, F-92150 Suresnes, France; and [e]Assistance Publique – Hôpitaux de Paris, Service d'Immunologie Biologique, Hôpital Européen Georges Pompidou, F-75015 Paris, France

Hemolytic diseases are frequently linked to multiorgan failure subsequent to vascular damage. Deciphering the mechanisms leading to organ injury upon hemolytic event could bring out therapeutic approaches. Complement system activation occurs in hemolytic disorders, such as sickle cell disease, but the pathological relevance and the acquisition of a complement-activating phenotype during hemolysis remain unclear. Here we found that intravascular hemolysis, induced by injection of phenylhydrazine, resulted in increased alanine aminotransferase plasma levels and NGAL expression. This liver damage was at least in part complement-dependent, since it was attenuated in complement $C3^{-/-}$ mice and by injection of C5-blocking antibody. We evidenced C3 activation fragments' deposits on liver endothelium in mice with intravascular hemolysis or injected with heme as well as on cultured human endothelial cells (EC) exposed to heme. This process was mediated by TLR4 signaling, as revealed by pharmacological blockade and TLR4 deficiency in mice. Mechanistically, TLR4-dependent surface expression of P-selectin triggered an unconventional mechanism of complement activation by noncovalent anchoring of C3 activation fragments, including the typical fluid-phase $C3(H_2O)$, measured by surface plasmon resonance and flow cytometry. P-selectin blockade by an antibody prevented complement deposits and attenuated the liver stress response, measured by NGAL expression, in the hemolytic mice. In conclusion, these results revealed the critical impact of the triad TLR4/P-selectin/complement in the liver damage and its relevance for hemolytic diseases. We anticipate that blockade of TLR4, P-selectin, or the complement system could prevent liver injury in hemolytic diseases like sickle cell disease.

complement | heme | endothelium | P-selectin | TLR-4

Intravascular hemolysis is a hallmark of a large spectrum of pathologies, including socially significant diseases such as sickle cell disease (SCD) and malaria, characterized by the presence of a large amount of red blood cell (RBC) degradation products in the circulation (1, 2). Cell-free hemoglobin, heme, and RBC microvesicles act by different mechanisms to promote vascular and tissue injury (3). Heme is a danger-associated molecular pattern molecule, which recruits and activates neutrophils (4–6) and macrophages (7, 8), induces vasoconstriction (9), and activates endothelial cells (EC) (10, 11). Moreover, heme modulates the activity of different plasma systems (12), including the innate immune complement cascade (11, 13–17).

In hemolytic diseases, signs of complement system activation are detected in circulation, on RBC and on endothelium (18, 19), but the mechanisms and the pathological relevance are still not well understood (13, 20, 21). Heme triggers Toll-like receptor 4 (TLR4) signaling (7, 10) on EC, but the contribution of this innate immune receptor in transforming resting endothelium to a complement-activating surface is unclear. The liver is highly vascularized and impacted by hemolysis, being the second site of RBC fragment

clearance and hemoglobin and heme detoxification. Furthermore, hepatic involvement is observed in 10–40% cases of SCD crisis (22) and in models of hemolytic diseases (17, 23), but the contribution of complement system remains unexplored.

We describe a nonconventional mechanism of complement activation in hemolytic conditions. In it, the fluid-phase component $C3(H_2O)$ [or a $C3(H_2O)$-like form] binds to the EC membranes via P-selectin (P-sel), expressed after heme-triggered TLR4 signaling. Deficiency/blockade of complement, TLR4, P-sel, and heme attenuated the liver stress response in mice with intravascular hemolysis. These results revealed the critical impact of the triad TLR4/P-sel/complement in the liver injury under hemolytic conditions and its relevance for hemolytic diseases.

Results

C3 Activation Fragments Are Deposited on Vascular Endothelium in the Liver of Mouse Models of Intravascular Hemolysis. Well-characterized models for heme injection and phenylhydrazine (PHZ)-induced intravascular hemolysis (20, 24) were used to determine to what extent hemolysis is responsible for complement deposits in the liver. We used an antibody (Ab), detecting

Significance

Complement system activation occurs in sickle cell disease and other hemolytic disorders, but the pathological relevance and the acquisition of a complement-activating phenotype by host cells during hemolysis remain unclear. Here we demonstrated that intravascular hemolysis triggered liver damage, which was attenuated in C3-deficient mice or by C5 blockade, showing the importance of complement system for hemolysis-mediated tissue stress response. Heme-dependent complement deposits were detected on endothelium, appeared upon activation of TLR4, and were mediated by P-selectin. This resulted in unconventional complement activation, mediated by anchoring of $C3(H_2O)$ on endothelial surface. In conclusion, our data suggest that complement system could be a therapeutic target in hemolytic diseases, such as sickle cell disease.

the C3 activation fragments [C3b, iC3b, C3(H_2O)-like] but not native C3. Treatment with PHZ or heme significantly increased C3 activation fragments' deposition on endothelium in the liver, compared with PBS in WT mice (Fig. 1 *A* and *B*). The double-staining of C3 activation fragments/vWF was localized on macrovessels, mainly, central hepatic veins, as well as on liver sinusoids (*SI Appendix*, Fig. S1*A*), confirmed by colocalization with vascular CD31 (*SI Appendix*, Fig. S1*B*). Bile ducts were not impacted by complement activation, as shown by the absence of colocalization with an epithelial marker cytokeratine (*SI Appendix*, Fig. S1*C*). The C3 activation fragments' staining in the liver sinusoids colocalized with macrophages/Kupffer cells CD68 (*SI Appendix*, Fig. S1*D*), granulocytes/neutrophils Ly6G (*SI Appendix*, Fig. S1*E*), and with platelets' marker CD41a (*SI Appendix*, Fig. S1*F*). The presence of neutrophils and platelets here supports the concept that complement plays a critical role in the induction of platelet–neutrophil aggregates on endothelium (25).

As expected, no C3 activation fragments' deposits were detected in C3$^{-/-}$ mice treated with PHZ (*SI Appendix*, Fig. S2). Importantly, in TLR4$^{-/-}$ mice, the complement deposits on vessels were strongly reduced, compared with WT mice, despite treatments (Fig. 1 *A* and *B*). These vascular deposits were attenuated by injection of heme scavenger hemopexin (Hx) in WT mice (Fig. 1*C*).

Complement Activation and TLR4 Signaling Triggered by Heme Contribute to the Hemolysis-Induced Liver Stress Response. We detected signs of liver injury in PHZ-treated mice by measuring plasmatic alanine aminotransferase (ALT) levels, which were significantly decreased in TLR4$^{-/-}$ and C3$^{-/-}$ hemolytic mice (Fig. 2 *A* and *B*). Of note, basal ALT activity weakly but significantly increased in C3$^{-/-}$ compared with WT mice.
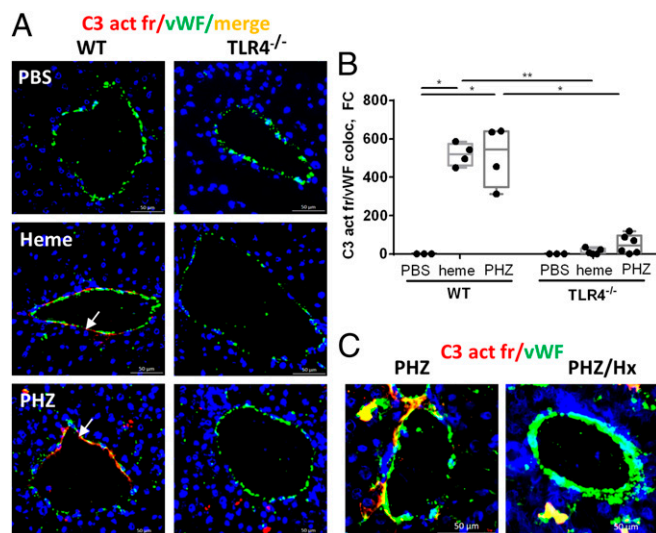

Fig. 1. Pattern of staining for C3 activation fragments in the liver of mice with intravascular hemolysis and their dependence on TLR4 and heme. (*A* and *B*) C3 fragments' deposition on vascular endothelium. (*A*) Double-staining for vWF (green) and C3b/iC3b (red) of WT and TLR4$^{-/-}$ mice liver frozen sections treated with PBS, heme, or PHZ. Colocalization is in orange. Focus on macrovessels, in particular, central hepatic veins. White arrows point to C3 activation fragments' deposition along endothelium. (*B*) Staining quantification, presented as fold change (FC) of the double-positive C3 activation fragments (C3 act fr)/vWF area of each liver section, normalized to the staining of the PBS-injected group of the WT mice. Comparison of WT and TLR4$^{-/-}$ ($n \geq 3$) mice. *$P < 0.05$, **$P < 0.005$; two-way ANOVA with Tukey's test for multiple comparisons. (*C*) Frozen liver sections of WT mice, treated with PHZ ± Hx, were stained for vWF (green) and C3 activation fragments (red).
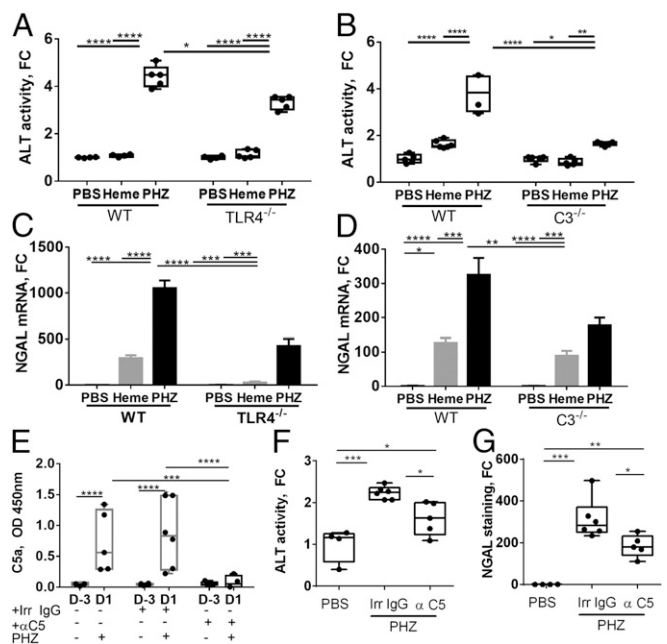

Fig. 2. Hemolysis triggers liver injury in a TLR4- and complement-dependent manner. WT, TLR4$^{-/-}$, and C3$^{-/-}$ mice were injected with PBS, heme, or PHZ. Livers were recovered after 24 h. (*A*) ALT activity was measured in WT and TLR4$^{-/-}$ mice, presented as fold change (FC), compared with the PBS group ($n \geq 4$). (*B*) ALT activity was measured in WT and C3$^{-/-}$ mice ($n \geq 3$). (*C*) Gene expression of NGAL in livers from WT and TLR4$^{-/-}$ mice, FC ($n \geq 4$). (*D*) Gene expression of NGAL in livers from WT and C3$^{-/-}$ mice, FC ($n \geq 3$). (*E*–*G*) Efficacy of C5 blockade to prevent liver injury. (*E*) C5a levels in the plasma of mice, injected with PHZ or pretreated with irrelevant IgG (Irr IgG) or anti–C5-blocking Ab BB5.1 (α-C5). The levels of C5a are compared at day 3 (D-3) and day 1 (D-1) post PHZ injection. The prevention of C5a release indicated that the Ab exerted its blocking effect ($n \geq 4$). (*F*) ALT activity levels (FC) or (*G*) quantification of the percentage of NGAL positive area in the liver (FC) in the mice, injected with PBS or PHZ, pretreated with Irr IgG or anti-C5. *$P < 0.05$, **$P < 0.005$, ***$P < 0.001$, ****$P < 0.0001$; two-way ANOVA with Tukey's test for multiple comparisons. Values are box plots with median and Min/Max points in *A*, *B*, and *E*–*G*, and mean ± SEM in *C* and *D*.

Further, we studied hypoxic cellular stress response protein NGAL, a sensitive marker for acute liver injury (26–28), upregulated in the liver in models of intravascular hemolysis and hypoxia by hepatocytes, neutrophils, Kupffer cells, and EC (29). Moreover, NGAL expression could be induced in a TLR4-dependent manner (26, 30). The expression of NGAL in WT mice injected with PHZ strongly increased at mRNA, and protein level and was attenuated in TLR4$^{-/-}$ and C3$^{-/-}$ hemolytic mice (Fig. 2 *C* and *D* and *SI Appendix*, Fig. S3*A*). NGAL up-regulation was reproduced by injection of heme at different regiments (weak effect with 40 µmol/kg i.v. and strong effect with two i.p. injections; Fig. 2 *C* and *D* and *SI Appendix*, Fig. S3*A*). Of note, i.v. injection of 100 µmol/kg of heme was lethal. Therefore, the i.p. injection was selected for the rest of the study, since it was well-tolerated by the mice (24, 31) and triggered complement deposits (Fig. 1 *A* and *B*). The heme-mediated NGAL expression was attenuated by pretreatment with Hx (*SI Appendix*, Fig. S3*B*). The NGAL staining in hemolytic mice was with punctiform appearance in the liver sinusoids (likely the EC and Kupffer cells) as well as on macrovessel walls in WT mice (ramification of hepatic arteries, portal veins, and central hepatic veins), while in TLR4$^{-/-}$, only a fraction of the sinusoidal staining was detected with no signal in the macrovessels.

Having shown the contribution of the C3 activation fragments in the liver injury, we studied the role of C5a and C5b-9. No staining for C5b-9 was detected in the liver sections of PHZ-injected mice. Nevertheless, C5a showed increased plasmatic

levels 24 h after PHZ injection (Fig. 2*E*). To find out if C5a contributes to the pathological process, we injected C5-blocking Ab BB5.1 [known to prevent mouse C5 cleavage (32)], which prevented the C5a generation (Fig. 2*E*). The treatment resulted in a partial decrease of the ALT levels (Fig. 2*F*). The NGAL liver staining by immunofluorescence (IF) showed significant decrease (Fig. 2*G* and *SI Appendix*, Fig. S3*C*), despite that there was no significant difference in NGAL mRNA levels (*SI Appendix*, Fig. S3*D*). As expected, the C3 activation fragments' deposits were not modified by BB5.1 (*SI Appendix*, Fig. S3*E*) Taken together, these results demonstrate the critical importance of the TLR4 signaling and complement activation at the level of C3 and, to a lesser extent, of C5 for the liver injury during intravascular hemolysis.

Heme Triggers TLR4 Activation on EC in Vitro. Having shown TLR4-dependent EC activation and complement deposits in presence of heme and hemolysis, we studied this process in vitro. TLR4 staining was positive on resting macrovascular EC (primary human umbilical vein endothelial cells, HUVEC) by flow cytometry (*SI Appendix*, Fig. S4*A*), as described for multiple EC, including of liver origin (33). After 30 min incubation with heme, TLR4-inhibitor TAK-242, or TLR4-ligand LPS, TLR4 expression remained stable (*SI Appendix*, Fig. S4 *B–D*). CD14 staining showed a double-peak on resting state, distributed at 50% of both dim (CD14^{low}) and bright cells (CD14^{high}) (*SI Appendix*, Fig. S4 *E* and *F*). Bright population of CD14 increased up to 80% after heme treatment, only partially prevented by TAK-242 (*SI Appendix*, Fig. S4*F*). LPS had no effect (*SI Appendix*, Fig. S4 *G* and *H*). The absence of TLR4 internalization [occurring in macrophages (34)] despite the rapid CD14 up-regulation from intracellular stores [as azurophilic granules of neutrophils (35, 36)] could be explained by the lack of TRAM in EC (37).

TLR4 activation was studied by phosphorylation of its signaling pathway intermediates and was in agreement with previous data (10). Phosphorylation of p-38 increased within 6 h with 25 μM of heme in a time-dependent manner, measured by IF (*SI Appendix*, Fig. S4*I*). Moreover, translocation of P-p65 in the nucleus increased up to 6 h, measured by Western blot and IF (*SI Appendix*, Fig. S4 *J* and *K*). Similarly, LPS induced an increase of the p38 and p65 phosphorylations. These results indicate that heme triggers TLR4 signaling on EC.

Inhibition of TLR4 Attenuates Heme-Induced Complement Deposits on EC. Our in vivo experiments suggested a direct link between the heme-mediated TLR4 signaling and the EC complement deposits. Therefore, we used an in vitro model, where exposure of EC to heme and normal human serum (NHS) resulted in an increase of C3 activation fragments and C5b-9 deposition within 30 min (*SI Appendix*, Fig. S5 *A* and *C*). This was associated with increased Bb release (1.8-fold at 100 μM heme, compared with medium), confirming the implication of the alternative pathway (AP) (11, 38). Inhibition of TLR4 by TAK-242 prevented about 50% of both C3 activation fragments and C5b-9 deposition (*SI Appendix*, Fig. S5 *B* and *D*). However, LPS treatment did not induce complement deposits (*SI Appendix*, Fig. S5 *E–H*). Moreover, the effect of heme was not related to LPS contamination, since the deposits on heme-exposed EC were unaffected despite preincubation with LPS-inhibitor Polymixin B (*SI Appendix*, Fig. S5 *I* and *J*).

To find out why LPS did not promote complement deposits in the studied conditions, we incubated different doses of heme or LPS in NHS. At 2 μM, LPS did not trigger complement activation, as measured by release of Bb or sC5b-9 (*SI Appendix*, Fig. S5 *K* and *L*). In contrast, exposure to 100 μM resulted in release of Bb and sC5b-9 from both LPS and heme (*SI Appendix*, Fig. S5 *K* and *L*).

Inhibition of TLR4 Does Not Impact the Expression/Binding of Complement Regulators and Receptors. A defect of complement regulation subsequent to TLR4 activation by heme could explain the partial protective effect of TAK-242 against complement deposition on EC. Thus, we studied the impact of heme treatment on the factor H (FH) binding on EC and the membrane cofactor protein (MCP, CD46) expression, the two major complement regulators, as well as the expression of C3a and C5a receptors (C3aR and C5aR, respectively) within 30 min.

Binding of FH increased on EC surface in presence of heme and was not prevented by TAK-242 (*SI Appendix*, Fig. S6 *A* and *B*). Heme caused a dose-dependent decrease of MCP (up to 50%), in agreement with Frimat et al. (11), which was not prevented by TAK-242 (*SI Appendix*, Fig. S6 *C* and *D*). Treatment with LPS did not modulate FH binding or MCP expression (*SI Appendix*, Fig. S7 *A–D*).

To find out whether the down-regulation of MCP contributes to the complement deposits on heme-exposed EC, we performed gene silencing, which reduced the expression of MCP to up to 80% (*SI Appendix*, Fig. S6 *G* and *H*). Upon exposure to heme, the EC with silenced MCP presented more C3 activation fragments' deposition, compared with a control siRNA (*SI Appendix*, Fig. S6 *G* and *H*).

Expression of both C3aR and C5aR revealed a double-peak on resting state, distributing 50% of dim and bright cells. Heme treatment rapidly increased both C3aR and C5aR expressions, enhancing the bright cell population (*SI Appendix*, Fig. S6 *I–L*). However, neither C3aR- nor C5aR-increased expression was prevented by TAK-242 (*SI Appendix*, Fig. S6 *I–L*). In comparison, LPS treatment did not affect C3aR and C5aR (*SI Appendix*, Fig. S7 *E–H*). These data point toward a second mechanism, mediating complement activation on human EC, which is independent on TLR4 and related to the expression of complement regulators.

A Rapid Increase of P-Sel Expression Is the Causal Link Between TLR4 and Complement Activation in Presence of Heme on EC in Vitro. P-sel expression induced by heme could participate in complement deposition on EC (39). First, we observed that both LPS and heme induced Weibel Palade bodies (WPB) mobilization within 30 min, translated by the release of vWF and the rapid expression of P-sel (*SI Appendix*, Fig. S8 *A–F*). We did not detect properdin binding on EC (*SI Appendix*, Fig. S8 *E* and *F*).

Staining of C3b and P-sel by IF on HUVEC revealed a colocalization in the presence of heme (*SI Appendix*, Fig. S9*A*). Investigation of the interaction between C3b and P-sel by SPR gave a K_d of about 100 nM (Fig. 3*A*). Moreover, C3(H$_2$O) was also able to bind recombinant P-sel (Fig. 3*B*). Presence of heme did not affect the binding of both C3b and C3(H$_2$O) on P-sel (*SI Appendix*, Fig. S9 *B* and *C*). C3(H$_2$O) was detected noncovalently bound to heme-exposed EC, as acidic wash abolished C3a staining (Fig. 3*C*). The acidic wash reduced the C3 fragments binding to the same level as did the preincubation with TAK242, showing that the noncovalent binding was TLR-4–dependent (Fig. 3*D*).

To understand whether these interactions have functional consequences on EC, we tested the capacity of a blocking Ab against P-sel to prevent complement deposition. Blocking of P-sel prevented 50% of C3 fragments' deposition, compared with cells treated with an irrelevant Ab. This inhibition was equivalent to TLR4 blocking by TAK-242, and no additive effects of TAK-242 and Ab against P-sel were observed (Fig. 3 *E* and *F*).

P-Sel Blockade Attenuates Complement Deposits and Liver Stress Response in Vivo. Finally, to test the hypothesis that P-sel is responsible for the complement deposits in vivo, we pretreated the WT mice with blocking anti–P-sel Ab, followed by heme or PHZ. This treatment prevented liver stress response in the PHZ-treated mice, as measured by the decrease of NGAL protein

Fig. 3. P-selectin is induced secondary to heme-mediated TLR4 activation and serves as an anchoring platform for C3 activation fragments. (*A* and *B*) Interactions between C3b/P-selectin and C3(H_2O)/P-selectin were studied by surface plasmon resonance by injecting increased concentration of C3b (*A*) or freeze/thaw native C3 (*B*) on P-selectin–coated chip. (*C* and *D*) HUVEC were treated with 100 μM of heme and exposed to 33% NHS for 30 min at 37 °C. Cells were detached, washed 3× at pH 7.2 or pH 2.5, and stained for C3a (*C*) or C3 activation fragments (C3 act fr) (*D*) deposition. (*E* and *F*) HUVEC were treated with 100 μM of heme ± 400 nM of TAK-242 ± irrelevant Ab (irr Ig) or anti–P-selectin Ab (αP-sel) for 30 min at 37 °C and exposed to 33% NHS (with 10 mM EGTA and 2 mM MgCl2) for 30 min at 37 °C. Cells were detached and stained for C3 activation fragments' deposition (n > 5, flow cytometry). *$P < 0.05$, **$P < 0.005$, ***$P < 0.001$, ****$P < 0.0001$; two-way ANOVA with Tukey's test for multiple comparisons. Values are box plots with median and Min/Max points. FC, fold change, compared with basal level.

staining (*SI Appendix*, Fig. S10 *A*–*C*) and mRNA expression (Fig. 4*A*). This indicates that the injected dose shows some efficiency, despite that it did not rescue the ALT levels (*SI Appendix*, Fig. S11). Importantly, this P-sel blockade prevented complement deposits on liver endothelium in PHZ- and heme-treated WT mice (Fig. 4 *B* and *C*), both on large vessels (Fig. 4*D*, *Left*) and on liver sinusoids (Fig. 4*D*, *Right*). Together, the in vitro and in vivo data demonstrate that the P-sel expression is a causal link between TLR4 and complement activation during intravascular hemolysis.

Discussion

Here we demonstrate that intravascular hemolysis triggers complement-dependent liver injury. We found a direct link between heme-triggered TLR4 signaling on endothelium and complement system activation (*SI Appendix*, Fig. S12). These complement deposits are mediated by P-sel expression, causing recruitment of C3b and C3(H_2O) [or a heme-promoted C3(H_2O)-like form] on the cell surface. TLR4 signaling-mediated complement activation triggers liver stress response in hemolytic conditions, relevant for SCD.

Despite the clear evidence of complement activation in hemolytic diseases, its pathological relevance remains unclear. After hemolysis induction, C3 activation fragments' deposits occurred on liver endothelium and in the sinusoidal vessels. Moreover, the increase of the ALT levels and the overexpression of the inflammation and cell damage marker NGAL were largely prevented in $C3^{-/-}$ mice. The terminal pathway was also activated, as measured by up-regulation of plasmatic C5a, despite the lack of detectable C5b-9 deposits in the liver. At least in part the liver injury was C5-dependent, since ALT and NGAL staining partially decreased after blockade of C5. These results place complement, and especially the C3 activation fragments, as a key mediator of liver tissue damage in hemolytic conditions, such as SCD.

The process behind the acquisition of complement-activating phenotype by the endothelium is not well understood. Although predominant in the kidney, this phenomenon is not restricted to glomerular microvasculature (20) and is detected on liver endothelium of heme-injected mice (31) and here in mice with PHZ-induced hemolysis. Here we establish that the complement deposits on endothelium are mediated by TLR4 and triggered by the TLR4 ligand heme. Furthermore, TLR4 deficiency partially prevented the liver stress response in our hemolysis model. Our results support the findings of Bozza and coworkers (7) for the involvement of TLR4 in heme sensing under hemolytic conditions, here in a system exempt from certain heme-related artifacts occurring in vitro (40). Further, we investigated the molecular and cellular mechanism explaining complement activation on EC under hemolytic conditions.

Belcher et al. (10) demonstrated that heme triggers EC activation and WPB mobilization via TLR4. Both P-sel (39, 41) and

Fig. 4. P-selectin blockade prevents complement deposits and liver stress response in mice with intravascular hemolysis. Anti–P-selectin administration prevents complement activation on endothelium and increases of liver injury marker NGAL in hemolytic conditions. WT mice were injected with PBS, heme, or PHZ after first administration of an irrelevant (Irr Ig) or blocking Ab against P-selectin (αP-sel). (*A*) Gene expression of NGAL in livers. (*B* and *C*) Staining quantification (n ≥ 4) for vascular C3 activation fragments' deposits (C3 act fr) (*B*) after injection of heme or (*C*) after induction of hemolysis by PHZ. (*D*) Examples of double-staining for vWF (green) and C3 activation fragments (red) of liver frozen sections by IF after PHZ injection. Focus on macrovessels, in particular central hepatic veins (*Left*) and on sinusoidal capillaries (*Right*). White arrows point to colocalization between C3 activation fragments and vWF (orange). *$P < 0.05$, ****$P < 0.0001$; two-way ANOVA with Tukey's test for multiple comparisons. Values are represented as mean ± SEM in *A* and box plots with median and Min/Max points in *B* and *C*. FC, fold change, compared with PBS-injected mice.

vWF (42, 43) modulate complement activation. P-sel promotes anchoring of C3b to EC membrane (39, 41), and, indeed, here we detected C3b/P-sel interaction. Together with the covalent and noncovalent binding of C3b to the cell surface, we found a noncovalent attachment of C3(H$_2$O) [or a heme-promoted C3(H$_2$O)-like form] to heme-exposed EC. C3(H$_2$O) is the fluid-phase activation product of C3, critical for the so called "tick over" of the AP (44). Here we discovered a nonconventional mechanism of complement deposits triggering the AP, where P-sel is expressed on heme-treated EC surface via TLR4-mediated process and serves as a platform for C3(H$_2$O) attachment. This explains why C3(H$_2$O) was found on heme-exposed EC membrane. Another platform molecule for recruitment of C3 fragments is properdin (45, 46), but we did not detect it on heme-exposed EC. Here, blocking P-sel/C3 activation fragments' interaction drastically reduced complement activation and the endothelium injury. Together, these results demonstrate a central role of P-sel to tag endothelium as a target for complement activation in vivo and provide the missing link between TLR4 and complement activation. This phenomenon is of a particular relevance, since P-sel is a critical player in the vaso-occlusion process of SCD patients (47–50). Indeed, P-sel–inhibitor crizanlizumab was associated with a lower frequency of sickle cell-related pain crises in patients (51). Complement activation is also observed in SCD (52–54), and its blockade prevents stasis in a mouse model (55). Therefore, we postulate that a P-sel blockade will reduce complement activation on endothelium of SCD patients and therefore the complement-mediated endothelial lesions.

At the trace amount used, sufficient for signaling pathway activation and P-sel expression, as shown here and described for microvascular EC (56) and in mice (41), LPS failed to induce complement activation. Only very high doses of LPS were able to activate complement, in line with previous works performed in vitro (57, 58) and in vivo (59). In contrast, heme has a higher ability to promote complement activation on EC. This disparity with LPS lies in the capacity of heme to bind C3 and to generate C3(H$_2$O) (11). The concomitant expression of P-sel and C3(H$_2$O) generation by heme may explain its capacity to activate complement on endothelium in our model.

Our in vitro results indicate that TLR4 stimulation is not the only mechanism contributing to complement-activating phenotype of heme-exposed human EC, while it is dominant in mice. The loss of MCP contributes to the C3 activation fragments' deposits in a TLR4-independent way, as seen on the MCP-silenced, heme-exposed EC. The decreased MCP levels will hamper the inactivation of C3b to iC3b, promoting this generation of novel convertases. FH binds to the heme-exposed cells to strengthen this regulatory capacity, but is not sufficient to compensate the regulatory function in case of severe MCP loss. Of note, mice lack expression of MCP on EC, pointing to the species differences in the mechanism of complement regulation on endothelium (60), and might explain the dominant effect observed in mice. In the mouse model, the complement activation by RBC microvesicles and the hypoxia-mediated cell and tissue injury during hemolysis could account for the TLR-4–independent, complement-dependent part of the liver injury.

C3aR and C5aR were rapidly up-regulated on EC in a TLR4-independent manner, most likely through exocytosis from still unidentified granules, different from WPB (61) and likely related to lysosomes, as in T-cells (20). Heme triggers C3a and C5a release in serum and on EC surface (11), and we detected it in the plasma of PHZ-injected mice. This could induce C3aR and C5aR signaling and the subsequent amplification of complement deposits (41, 61). C3a and C5a are potent proinflammatory mediators, playing a key role in vascular and tissue injury (19). Hemolysis, TLR4 signaling, and the complement anaphylatoxins would synergize to trigger vascular stress response and tissue damage in hemolytic diseases. Moreover, the liver injury is a complex process. Additional hemolysis-derived factors or the ischemia/reperfusion injury are also well known for activating complement system and for involving TLR4. Heme could synergize also with other endogenous TLR4 ligands, which could be released during hemolysis, such as HMGB1 (62, 63), and could contribute to the liver injury and stress response. RBC microvesicles, activating complement and carrying adhesive C3b deposits, as well as hemoglobin-mediated effects through NO scavenging, contribute to these hemolysis-mediated pathologic effects (64, 65).

In conclusion, our study demonstrated that complement triggers tissue injury during intravascular hemolysis by an acquisition of a heme-dependent, complement-sensitive activated phenotype by endothelium (*SI Appendix*, Fig. S12). The sequence of reactions involves: (*i*) heme-mediated signaling through TLR4, (*ii*) P-sel expression, and (*iii*) interaction of C3b and C3(H$_2$O). This process triggers the amplification loop of the AP, generating local inflammation. This mechanism could operate at any type of endothelium, since EC generally express TLR4. On the basis of these results, targeted therapies on heme, TLR4 pathway, or P-sel could prevent organ dysfunction in hemolytic diseases, including by limiting complement activation. Moreover, complement appears as a therapeutic target, at C3 level and to some extent at C5 level, to prevent organ injury in hemolytic diseases.

Materials and Methods

For fully detailed procedures, please refer to *SI Appendix, Methods*.

Mouse Treatment. All experiments were conducted in accordance with the recommendations for the care and use of laboratory animals and with the approval, APAFIS#7135–2016100520465430v5, of the French Ministry of Agriculture. Eight-week-old C57BL/6, C3$^{-/-}$, and TLR4$^{-/-}$ mice were injected i.p. with 100 μL of PBS, freshly prepared heme [40 μmol/kg (10)], or with PHZ (900 μmol/kg). In a set of experiments, mice were pretreated with i.p. injection of 40 μmol/kg of human Hx 1 h before heme or PHZ injection. Blocking Ab against P-selectin, anti-C5, or their isotype controls was administered in a set of experiments.

mRNA Level Analyses. Snap-frozen liver sections were recovered in RLT buffer (Qiagen)+ 1% β-mercaptoethanol and used for mRNA extraction and gene expression analyzed by RT-qPCR as described (24). NGAL expression was normalized by actin.

IF. Five-micrometer-thick frozen sections of mouse livers were stained for C3 activation fragments or NGAL. Colocalization with vWF staining was used to quantify the complement deposits on vascular endothelium in the liver as percent of double-positive area, expressed as FC.

Cell Culture and Gene Silencing. HUVEC from healthy donors were collected after informed consent (authorization number: DC-2008-642, CHRU de Lille) and studied by flow cytometry. At 80% confluency, HUVEC were transfected in Opti-MEM medium supplemented with lipotransfectamine and 4 nM of MCP siRNA for 20 min at RT.

ALT Activity Quantification. ALT activity in mouse plasma was quantified using a colorimetric assay, expressed in nmol/min/μL following the protocol provided by the manufacturer.

Surface Plasmon Resonance. Binding studies were performed using the ProteOn XPR36. Recombinant human P-selectin was covalently coupled to a sensor chip. Interactions were measured with increased concentration of C3b and C3(H$_2$O).

1. Deuel JW, et al. (2015) Different target specificities of haptoglobin and hemopexin define a sequential protection system against vascular hemoglobin toxicity. *Free Radic Biol Med* 89:931–943.
2. Dutra FF, Bozza MT (2014) Heme on innate immunity and inflammation. *Front Pharmacol* 5:115.
3. Rother RP, Bell L, Hillmen P, Gladwin MT (2005) The clinical sequelae of intravascular hemolysis and extracellular plasma hemoglobin: A novel mechanism of human disease. *JAMA* 293:1653–1662.
4. Chen G, et al. (2014) Heme-induced neutrophil extracellular traps contribute to the pathogenesis of sickle cell disease. *Blood* 123:3818–3827.
5. Graça-Souza AV, Arruda MAB, de Freitas MS, Barja-Fidalgo C, Oliveira PL (2002) Neutrophil activation by heme: Implications for inflammatory processes. *Blood* 99:4160–4165.
6. Porto BN, et al. (2007) Heme induces neutrophil migration and reactive oxygen species generation through signaling pathways characteristic of chemotactic receptors. *J Biol Chem* 282:24430–24436.
7. Figueiredo RT, et al. (2007) Characterization of heme as activator of Toll-like receptor 4. *J Biol Chem* 282:20221–20229.
8. Vinchi F, et al. (2016) Hemopexin therapy reverts heme-induced proinflammatory phenotypic switching of macrophages in a mouse model of sickle cell disease. *Blood* 127:473–486.
9. Nath KA, et al. (2018) Role of TLR4 signaling in the nephrotoxicity of heme and heme proteins. *Am J Physiol Renal Physiol* 314:F906–F914.
10. Belcher JD, et al. (2014) Heme triggers TLR4 signaling leading to endothelial cell activation and vaso-occlusion in murine sickle cell disease. *Blood* 123:377–390.
11. Frimat M, et al. (2013) Complement activation by heme as a secondary hit for atypical hemolytic uremic syndrome. *Blood* 122:282–292.
12. Roumenina LT, Rayes J, Lacroix-Desmazes S, Dimitrov JD (2016) Heme: Modulator of plasma systems in hemolytic diseases. *Trends Mol Med* 22:200–213.
13. Pawluczkowycz AW, Lindorfer MA, Waitumbi JN, Taylor RP (2007) Hematin promotes complement alternative pathway-mediated deposition of C3 activation fragments on human erythrocytes: Potential implications for the pathogenesis of anemia in malaria. *J Immunol* 179:5543–5552.
14. Dimitrov JD, Roumenina LT, Doltchinkova VR, Vassilev TL (2007) Iron ions and haeme modulate the binding properties of complement subcomponent C1q and of immunoglobulins. *Scand J Immunol* 65:230–239.
15. Roumenina LT, et al. (2011) Heme interacts with c1q and inhibits the classical complement pathway. *J Biol Chem* 286:16459–16469.
16. Lindorfer MA, et al. (2016) Compstatin Cp40 blocks hematin-mediated deposition of C3b fragments on erythrocytes: Implications for treatment of malarial anemia. *Clin Immunol* 171:32–35.
17. Hanson MS, et al. (2013) A novel hemoglobin-binding peptide reduces cell-free hemoglobin in murine hemolytic anemia. *Am J Physiol Heart Circ Physiol* 304:H328–H336.
18. Merle NS, Church SE, Fremeaux-Bacchi V, Roumenina LT (2015) Complement system part I–Molecular mechanisms of activation and regulation. *Front Immunol* 6:262.
19. Merle NS, Noe R, Halbwachs-Mecarelli L, Fremeaux-Bacchi V, Roumenina LT (2015) Complement system part II: Role in immunity. *Front Immunol* 6:257.
20. Le Friec G, et al. (2012) The CD46-Jagged1 interaction is critical for human TH1 immunity. *Nat Immunol* 13:1213–1221.
21. Koethe SM, Casper JT, Rodey GE (1976) Alternative complement pathway activity in sera from patients with sickle cell disease. *Clin Exp Immunol* 23:56–60.
22. Shah R, Taborda C, Chawla S (2017) Acute and chronic hepatobiliary manifestations of sickle cell disease: A review. *World J Gastrointest Pathophysiol* 8:108–116.
23. Wandersee NJ, Holzhauer SL, Retherford DM, Foster TD, Hillery CA (2014) Evidence for transient acute liver injury in mouse models of sickle cell disease during steady state health. *Blood* 124:1373.
24. Merle NS, et al. (2018) Characterization of renal injury and inflammation in an experimental model of intravascular hemolysis. *Front Immunol* 9:179.
25. Riedl M, et al. (2016) Complement activation induces neutrophil adhesion and neutrophil-platelet aggregate formation on vascular endothelial cells. *Kidney Int Rep* 2:66–75.
26. Yoshikawa K, et al. (2017) Neutrophil gelatinase-associated lipocalin level is a prognostic factor for survival in rat and human chronic liver diseases. *Hepatol Commun* 1:946–956.
27. Ariza X, et al.; CANONIC Investigators, EASL CLIF Consortium (2016) Neutrophil gelatinase-associated lipocalin is a biomarker of acute-on-chronic liver failure and prognosis in cirrhosis. *J Hepatol* 65:57–65.
28. Xu M-J, et al. (2015) Liver is the major source of elevated serum lipocalin-2 levels after bacterial infection or partial hepatectomy: A critical role for IL-6/STAT3. *Hepatology* 61:692–702.
29. Jiang W, Constante M, Santos MM (2008) Anemia upregulates lipocalin 2 in the liver and serum. *Blood Cells Mol Dis* 41:169–174.
30. Sunil VR, et al. (2007) Acute endotoxemia is associated with upregulation of lipocalin 24p3/Lcn2 in lung and liver. *Exp Mol Pathol* 83:177–187.
31. May O, et al. (2018) Heme drives susceptibility of glomerular endothelium to complement overactivation due to inefficient upregulation of heme oxygenase-1. *Front Immunol* 9:3008.
32. Wang Y, Rollins SA, Madri JA, Matis LA (1995) Anti-C5 monoclonal antibody therapy prevents collagen-induced arthritis and ameliorates established disease. *Proc Natl Acad Sci USA* 92:8955–8959.
33. Jagavelu K, et al. (2010) Endothelial cell toll-like receptor 4 regulates fibrosis-associated angiogenesis in the liver. *Hepatology* 52:590–601.
34. Zanoni I, et al. (2011) CD14 controls the LPS-induced endocytosis of Toll-like receptor 4. *Cell* 147:868–880.
35. Detmers PA, et al. (1995) Endotoxin receptors (CD14) are found with CD16 (Fc gamma RIII) in an intracellular compartment of neutrophils that contains alkaline phosphatase. *J Immunol* 155:2085–2095.
36. Rodeberg DA, Morris RE, Babcock GF (1997) Azurophilic granules of human neutrophils contain CD14. *Infect Immun* 65:4747–4753.
37. Harari OA, Alcaide P, Ahl D, Luscinskas FW, Liao JK (2006) Absence of TRAM restricts Toll-like receptor 4 signaling in vascular endothelial cells to the MyD88 pathway. *Circ Res* 98:1134–1140.
38. Merle NS, et al. (2018) Intravascular hemolysis activates complement via cell-free heme and heme-loaded microvesicles. *JCI Insight* 3:96910.
39. Del Conde I, Crúz MA, Zhang H, López JA, Afshar-Kharghan V (2005) Platelet activation leads to activation and propagation of the complement system. *J Exp Med* 201:871–879.
40. Vallelian F, et al. (2018) Revisiting the putative role of heme as a trigger of inflammation. *Pharmacol Res Perspect* 6:e00392.
41. Morigi M, et al. (2011) Alternative pathway activation of complement by Shiga toxin promotes exuberant C3a formation that triggers microvascular thrombosis. *J Immunol* 187:172–180.
42. Feng S, Liang X, Kroll MH, Chung DW, Afshar-Kharghan V (2015) Von Willebrand factor is a cofactor in complement regulation. *Blood* 125:1034–1037.
43. Noone DG, et al. (2016) Von Willebrand factor regulates complement on endothelial cells. *Kidney Int* 90:123–134.
44. Lachmann PJ, Lay E, Seilly DJ (2017) Experimental confirmation of the C3 tickover hypothesis by studies with an Ab (S77) that inhibits tickover in whole serum. *FASEB J* 32:123–129.
45. Saggu G, et al. (2013) Identification of a novel mode of complement activation on stimulated platelets mediated by properdin and C3(H2O). *J Immunol* 190:6457–6467.
46. Pedersen DV, et al. (2017) Functional and structural insight into properdin control of complement alternative pathway amplification. *EMBO J* 36:1084–1099.
47. Turhan A, Weiss LA, Mohandas N, Coller BS, Frenette PS (2002) Primary role for adherent leukocytes in sickle cell vascular occlusion: A new paradigm. *Proc Natl Acad Sci USA* 99:3047–3051.
48. Polanowska-Grabowska R, et al. (2010) P-selectin-mediated platelet-neutrophil aggregate formation activates neutrophils in mouse and human sickle cell disease. *Arterioscler Thromb Vasc Biol* 30:2392–2399.
49. Embury SH, et al. (2004) The contribution of endothelial cell P-selectin to the microvascular flow of mouse sickle erythrocytes in vivo. *Blood* 104:3378–3385.
50. Matsui NM, Varki A, Embury SH (2002) Heparin inhibits the flow adhesion of sickle red blood cells to P-selectin. *Blood* 100:3790–3796.
51. Ataga KI, et al. (2017) Crizanlizumab for the prevention of pain crises in sickle cell disease. *N Engl J Med* 376:429–439.
52. Mold C, Tamerius JD, Phillips G, Jr (1995) Complement activation during painful crisis in sickle cell anemia. *Clin Immunol Immunopathol* 76:314–320.
53. Strauss J, Pardo V, Koss MN, Griswold W, McIntosh RM (1975) Nephropathy associated with sickle cell anemia: An autologous immune complex nephritis. I. Studies on nature of glomerular-bound antibody and antigen identification in a patient with sickle cell disease and immune deposit glomerulonephritis. *Am J Med* 58:382–387.
54. Chudwin DS, Papierniak C, Lint TF, Korenblit AD (1994) Activation of the alternative complement pathway by red blood cells from patients with sickle cell disease. *Clin Immunol Immunopathol* 71:199–202.
55. Schaid TR, et al. (2016) Complement activation in a murine model of sickle cell disease: Inhibition of vaso-occlusion by blocking C5 activation. Available at www.bloodjournal.org/content/128/22/158?sso-checked=true. Accessed June 9, 2017.
56. Yin W, Ghebrehiwet B, Weksler B, Peerschke EIB (2008) Regulated complement deposition on the surface of human endothelial cells: Effect of tobacco smoke and shear stress. *Thromb Res* 122:221–228.
57. Brekke O-L, Christiansen D, Fure H, Fung M, Mollnes TE (2007) The role of complement C3 opsonization, C5a receptor, and CD14 in E. coli-induced up-regulation of granulocyte and monocyte CD11b/CD18 (CR3), phagocytosis, and oxidative burst in human whole blood. *J Leukoc Biol* 81:1404–1413.
58. Sprong T, et al. (2004) Complement activation and complement-dependent inflammation by Neisseria meningitidis are independent of lipopolysaccharide. *Infect Immun* 72:3344–3349.
59. Cunningham PN, et al. (2000) Complement is activated in kidney by endotoxin but does not cause the ensuing acute renal failure. *Kidney Int* 58:1580–1587.
60. Inoue N, et al. (2003) Disruption of mouse CD46 causes an accelerated spontaneous acrosome reaction in sperm. *Mol Cell Biol* 23:2614–2622.
61. Monsinjon T, et al. (2003) Regulation by complement C3a and C5a anaphylatoxins of cytokine production in human umbilical vein endothelial cells. *FASEB J* 17:1003–1014.
62. Yu L, Wang L, Chen S (2010) Endogenous toll-like receptor ligands and their biological significance. *J Cell Mol Med* 14:2592–2603.
63. Lin T, et al. (2012) Identification of hemopexin as an anti-inflammatory factor that inhibits synergy of hemoglobin with HMGB1 in sterile and infectious inflammation. *J Immunol* 189:2017–2022.
64. Reiter CD, et al. (2002) Cell-free hemoglobin limits nitric oxide bioavailability in sickle-cell disease. *Nat Med* 8:1383–1389.
65. Donadee C, et al. (2011) Nitric oxide scavenging by red blood cell microparticles and cell-free hemoglobin as a mechanism for the red cell storage lesion. *Circulation* 124:465–476.

IMMUNOLOGY AND INFLAMMATION